DUCTILE BEHAVIOUR OF OIL PALM SHELL CONCRETE SLABS SUBJECTED TO BLAST LOADS

U. Johnson Alengaram[1*], Nimasha H. W. Mohottige[2], Chengqing Wu[2], Mohd Zamin Jumaat[1], Yap Soon Poh[1], Zhongqi Wang[3]

[1]Centre for Innovative Construction Technology (CICT), Department of Civil Engineering, Faculty of Engineering, University of Malaya, 50603, Kuala Lumpur, Malaysia
e-mail: <johnson@um.edu.my>
[2]School of Civil, Environmental and Mining Engineering, the University of Adelaide, Australia
[3]State Key Laboratory of Explosion Science & Technology, Beijing Institute of Technology, Beijing, China

Abstract. Oil palm shell (OPS) is an industrial waste material abundantly available in Malaysia and other South East Asian countries. It has high aggregate impact resistance characteristics and hence its capability to withstand blast load was tested through OPS concrete (OPSC) slabs designed and developed in University of Malaya, Kuala Lumpur, Malaysia and tested at Huluduo, China. LVDTs, pressure transducers and accelerometers were used to record data of response of the slabs subjected to quasi-static load and blast loads of 1, 5 and 10 kg TNT. The recorded data were then analysed and compared and conclusions were made on the effectiveness of OPS as a coarse aggregate. It has been found that OPSC outperformed normal concrete (NC) slab when subjected to 10 kg TNT as OPSC panel was intact and had no shrapnel; the ductility behaviour of OPSC, it exhibited multiple cracks and the impact resistance of OPS through its energy absorption due to fibrous content within OPS itself was visible both in crack pattern and in its propagation. Though OPS is of organic nature, its resistance to blast waves was observed as the huge fire ball created due to blast had no or little effect on the OPSC panels.

Keywords: Oil palm shell, lightweight aggregate, oil palm shell concrete, blast load, blast resistance.

1. INTRODUCTION

Concrete is the most commonly used material in modern construction industry which is produced more than 10 billion tons each year worldwide [1]. And its demand is increasing due to expansion of population and radical development of infrastructure during the last 5 decades. It is expected that approximately 18 billion tons a year will be produced by 2050 [2]. However, the production of concrete and cement in huge volumes has an enormous impact on the environment as it consumes enormous amounts of natural resources; in addition, it causes severe environmental catastrophe during the manufacturing process [1, 3]. Thus, researchers and governments across the globe pumped huge amount of money and resources to finding alternatives to replace these natural resources. This has had positive impact as researchers focused on utilizing industrial by-products which are considered as wastes to produce environmental friendly concrete as sustainable alternatives [2, 4].

Malaysia is the second largest producers of palm oil in the world which generates 4 million tons of oil palm shell (OPS) annually as a waste material [5]. During the last two decades, a number of investigations have been conducted on utilizing OPS as an alternative lightweight coarse aggregate in the development of lightweight concrete which gives a desirable solution to deteriorating natural resources caused by overexploitation of granite aggregate and environmental pollution due to stockpile in the factory yards in open-air [5-8]. As a result, oil palm shell concrete (OPSC) has been developed by using OPS as coarse aggregate. Due to the low bulk density of OPS, OPSC has a density 20-25% lower than conventional concrete about 1900 kg/m^3 which makes it lightweight concrete (LWC) [6, 7]. LWC has several advantages over conventional concrete such as savings on reinforcement, formwork, scaffolding, foundation cost, etc. due to reduction of self-weight of structures and better heat insulation, sound absorption, frost resistance and anti-condensation properties [9]. One of the significant findings of OPS is its high resistance to impact due to fibrous contents; this has led to further investigation on its

resistance to impact loads. Unlike crushed granite aggregates, OPS have high resistance to impact-the fact that could be taken advantage of-as ductile behaviour of concrete is very much desired in structural elements. In addition, in structural elements subjected to impact and blast loads, the ductile behaviour of OPSC could be explored.

One of the most crucial components in blast-resistance structures is the selection of material in the concrete itself. Materials with good shock-absorbing characteristics have the potential to be utilized for improved ductility when subjected to impact forces and hence the enhanced blast resistance. Oil palm shell (OPS), which is a type of agricultural by-product, is known to exhibit lower aggregate impact value (AIV) than normal granite aggregates, and this indicates good shock-absorbing properties of the OPS [10]. The AIV value of OPS was reported to be in the range of 2 – 8% [5, 10, 11]. In lab-scale impact testing of panel specimens, it was found that concrete made with OPS lightweight aggregate had better impact resistance compared to high strength concrete and this was attributed to the lower AIV value and shape of the OPS aggregates [12]. In addition, the greater ductile behaviour of OPS concrete compared to conventional concrete was observed [13] and the major contributing factor of the ductility of OPS concrete is the low modulus of elasticity (MOE) of the resulting concrete. Similarly, [14] investigated the use of pumice aggregate concrete as buffer material for impact protection and found improved impact resistance of such concrete. In the study, the improved shock-absorbing performance of the pumice concrete was also credited to the lower MOE of the pumice concrete. [15] also echoed the suggestion of better shock-absorbing ability of lightweight concrete from investigations carried out on polystyrene aggregate concrete. According to the outcome of the research, the polystyrene aggregate concrete had improved impact resistance due to its low crushing strength and high degree of deformability or low MOE.

Addition of steel fibres is known to enhance the ductility performance of concrete, and this is of particular interest for structures subjected to blast and impact forces. While the improvement in blast and impact resistances of steel fibre reinforced normal weight concrete are known, there is little knowledge on the effect of steel fibre addition on the performances of OPS lightweight concrete. Even though lab-scale tests have shown the benefits for ductility enhancement of OPS concrete using the steel fibres [12, 16], there are no full-scale tests being carried out to evaluate its performance in terms of the blast resistance.

LWC has significantly low fracture toughness and tensile strength which makes it a brittle material. Hence recent research has focused on adding fibres into LWC so as to get better mechanical properties as well as to improve the ductility and flexural toughness [2-4]. Mo et al. [4] studied the effect of steel fibres on characteristics of OPSC and concluded that the effect of fibres in arresting the cracks and their propagation enhances the mechanical properties of OPSC such as compressive strength, splitting tensile strength and flexural tensile strength. Further they mentioned addition of 1.0% steel fibre improved the flexural toughness by up to 16 times and addition of 0.5% and 0.75% steel fibre enhanced the ductility by about 3 and 6 times, respectively [4].

There is a reasonable amount of research on static behaviour of OPSC. Teo et al. [5] and Mohammed et al. [6] studied the flexural behaviour of reinforced OPSC beams and concluded that the design equations in BS8110 can be used for prediction of the moment capacity of OPSC beams with up to certain amount of reinforcement ratio and the deflections and the crack widths are within the allowable limits and durability requirements given by BS8110. However, very limited research on dynamic behaviour of OPSC can be found. OPS has lower aggregate impact value than granite aggregate [7, 8]. This can be considered as an indication of high impact resistance of OPSC [9]. Kim et al. [12] conducted a research on impact resistance of OPSC and fibre reinforced OPSC and concluded that the final impact energy of OPSC and fibre reinforced OPSC exceeded the published results on high strength concrete. They also monitored that even after formation of the first crack, all OPSC specimens with and without fibre were able to sustain large amount of impact load before they failed [9].

Due to increment in accidental and intentional explosions, designing structures to resist explosion loads has been gained attention in recent years to minimise damages to valuable human lives and properties caused by structural failures [17-19]. OPSC is a material with good impact resistance. Thus, it is possible to make it an effective material for the construction of structures to resist blast and impact loadings. But little research has not been conducted to characterize blast resistance of OPSC structural elements.

To fill this gap, the University of Malaya jointly with Beijing Institute of Technology, Tianjin Chengjian University and the University of Adelaide conducted a series of quasi-static and blast tests on slabs with OPS used as a coarse aggregate. The concrete panels using OPS as coarse

aggregate was developed by Centre for Innovative Construction Technology (CICT), University of Malaya. The objective of the test program is to investigate the effectiveness of OPS as a lightweight coarse aggregate to replace granite aggregate in concrete when resisting static and blast loads. This paper discusses the results of this experiment program and conclusions are then made based on the results.

2. DESIGN OF EXPERIMENTS

In this experimental program, quasi-static (four point bending) and blast tests were performed on ten reinforced concrete slabs which were casted by three different types of concrete mixes including Normal Concrete (NC), and Oil Palm Shell Concrete (OPSC). Details of the material properties, design of the slab specimens and details of the experimental setups for both quasi-static and blast tests are discussed in this section.

2.1 Material Properties

All the concrete slabs were casted by Department of Civil Engineering, University of Malaya using locally available materials. Ordinary Portland cement which meets the ASTM: C150/C150 M-12 specifications, was used in all mix proportions. OPS obtained from an oil palm mill, has a compacted bulk density of 635 kg/m^3. It is 835 kg/m^3 lower than the crushed granite aggregates which was used in this study. Mining sand was used as the fine aggregate in all mixtures.

Table 1 presents composition of the concrete mixture used in the experimental program. Three concrete mixtures were manufactured including Grade 30 Normal Concrete (NC) as a control. OPS were used 100% as coarse aggregate in OPSC.

Table 1: Proportion of materials in the concrete mixtures in kg/m^3

Mix	Description	OPC	Silica Fume	Fine aggregate - Sand	Coarse Aggregate OPS	Coarse Aggregate Granite	Water	Super-plasticiser
1	Normal Concrete (NC)	322	0	677	0	1258	183	0
2	Oil Palm Shell Concrete (OPSC)	530	53	970	320	0	170	0.35

For each mix 100 mm cubes, 100mmϕ x 200 mm cylinders, 150mmϕ x 300 mm cylinders and 100mm x 100mm x 500 mm prisms were prepared to test for compressive strength (BS EN 12390-3:2009), splitting tensile strength (ASTM: C496/C496 M-11), modulus of elasticity/Poisson's ratio (ASTM: C469-10) and flexural strength (ASTM: C78-10) respectively [20]. After the de-moulding in 7 days, all the specimens were cured in water and tested at the age of 28-days.

Table 2 summarizes the mechanical properties of the concrete mixtures. It clearly shows that OPSC has density of 1950 kg/m^3 which is lesser than NC but when comparing compressive strengths it has a higher value than NC.

Table 2: Mechanical properties of the concrete mixtures

Mix	Description	Density (kg/m^3)	Compressive strength (MPa)	Splitting tensile strength (MPa)	Flexural strength (MPa)	Young's Modulus (GPa)	Poisson's ratio
1	Normal Concrete (NC)	2330	27.00	3.19	3.55	20.65	0.17
2	Oil Palm Shell Concrete (OPSC)	1950	38.50	3.08	3.79	12.25	0.28

2.2 Details of Slab Specimen

Totally, ten slabs were casted for both quasi-static and blast tests using three concrete mixtures. Three slabs for quasi-static tests and six slabs for blast tests, in total nine slabs were manufactured with dimensions of length 2.0m, width 1.0m and thickness 0.12m by NC, and OPSC. The details of the slab specimens are given in Table 3 including the steel reinforcement ratio used in each slab.

The reinforcement arrangement for all the slabs is shown in Figure 1. The slabs were constructed with 12 mm diameter reinforce steel bars which was spaced at 325 mm centres in the major bending plane and at 100 mm centres in the minor bending plane. The thickness of the concrete cover was 10 mm. The reinforcement had yield strength of 600 MPa, young's modulus of 200 GPa and fracture strain of 8%.

Table 3: Details of the slab specimens

No	Panel Name	Test	Dimensions (m)	Reinforcement ratio	Concrete Type
1	C1	Four point bending (static)	2.0 × 1.0 × 0.12	1.03%	Normal Concrete (NC)
2	C1A	Blast			
3	C1B				
4	C2	Four point bending (static)	2.0 × 1.0 × 0.12	1.03%	Oil Palm Shell Concrete (OPSC)
5	C2A	Blast			
6	C2B				

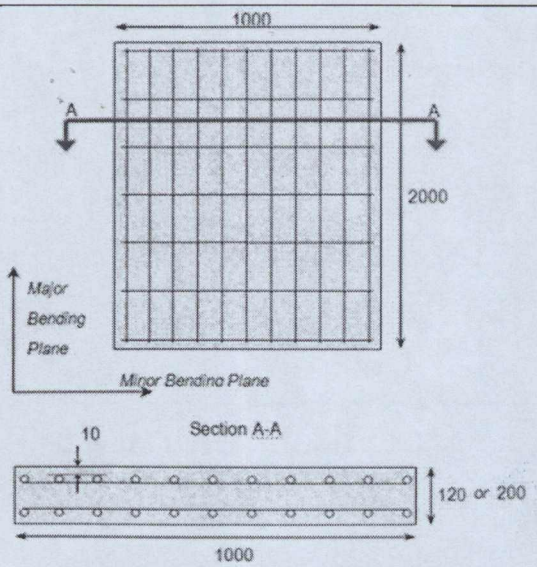

Figure 1: Reinforcement arrangement of the slabs

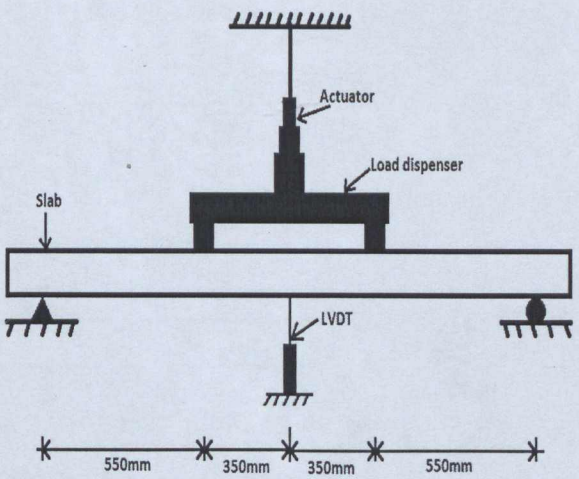

Figure 2: Four point bending test setup

2.3 Quasi-Static Tests

Four point bending tests were performed on three slabs to investigate their behaviours under quasi-static loads. The test set-up is shown in Figure 2. An actuator with 50 ton capacity was used to apply the loading on the slabs and two Linear Variable Displacement Transducers (LVDTs) which can measure up to 20 cm were utilized to record the mid-span deflection of the slabs. This test procedure followed the Chinese standards GB/T50152 (2012) for concrete test methods for standard structures.

2.4 Blast Tests

In total, ten blast events were performed on seven slabs. For each concrete type, 1 kg and 10 kg charge explosions were performed on the same slab by assuming slab response for 1 kg charge explosion is in elastic state. Table 4 gives all details about the blast events and the slab specimen which were utilized in this program.

For the blast events, scaled distance (= standoff distance/charge weight$^{1/3}$) was changed from 0.55 – 1.5 m/kg$^{1/3}$ by varying the charge weight from 1 - 20 kg while keeping the standoff distance (the distance between the charge and the slab) constant at 1.5 m. Data acquisition devices were installed to measure the reflected pressure-time, deflection-time and acceleration-time histories of the slabs.

Table 4: Details of the specimens and blast events

Event	Panel Name	Concrete Type	Standoff Distance (m)	Charge Weight (kg)	Scaled Distance (m/kg$^{1/3}$)
1	C1A	Normal Concrete (NC)	1.5	1	1.5
2			1.5	10	0.7
3	C1B		1.5	5	0.88
4	C2A	Oil Palm Shell Concrete (OPSC)	1.5	1	1.5
5			1.5	10	0.7
6	C2B		1.5	5	0.88

2.4.1 Experimental Setup

Each specimen was tested on a steel supporting frame which effectively provided an upward restraint against the slab's rebound to minimise any lateral movement as shown in Figure 3. Two railing posts were anchored to the ground and the charge was suspended from a wire, connecting the posts as per the figure. The standoff distance was measured from top face of the slab to the charge, which was suspended over the centre of the slab. 1 kg, 5 kg and 10 kg composition B explosives were used for this blast testing program. All the charges were in cylindrical shape. For all the experiments, the charge was hanged to face its circular face parallel to the span of the slab as shown in the figure.

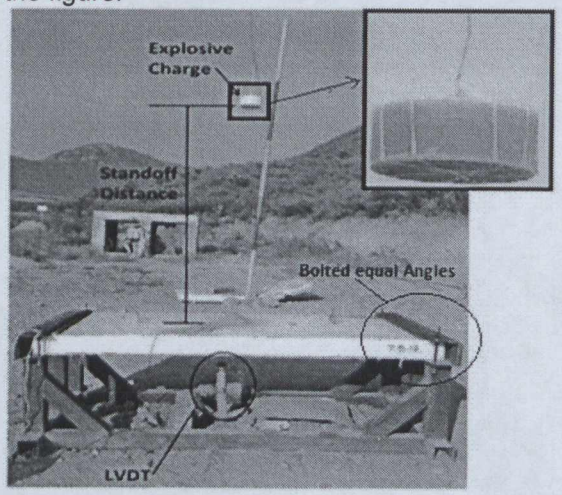

Figure 3: Support structure and explosive charge

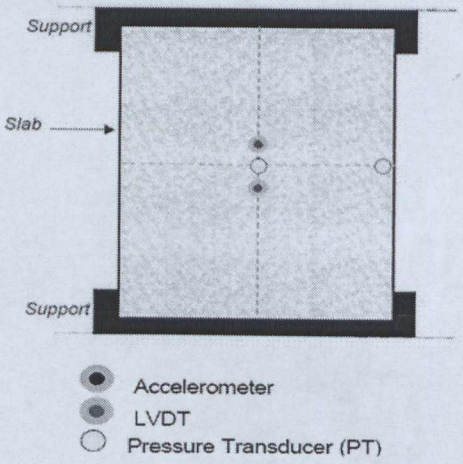

Figure 4: Slab instrumentation

2.4.2 Data Acquisition

Data acquisition devices used in this blast experiment program included LVDTs, Accelerometers and Pressure Transducers (PT). The LVDTs used for this testing program are able to measure up to 10 cm deflection and for accelerometers; the maximum tolerable acceleration is 50 m/s^2. The location of instrumentation can be seen in Figure 4. LVDT was installed at centre of the slab to measure the mid-span deflection. Accelerometer was also installed at the centre to verify the results of LVDT. Two Pressure Transducers were installed at centre of the slab and midpoint of the edge to measure the pressure-time histories over the slab.

3. EXPERIMENT RESULTS

3.1 Quasi-static test results

Force and deflection of the slabs were measured for all NC, and OPSC slabs. Figure 5 shows load-displacement relationships of the slabs.

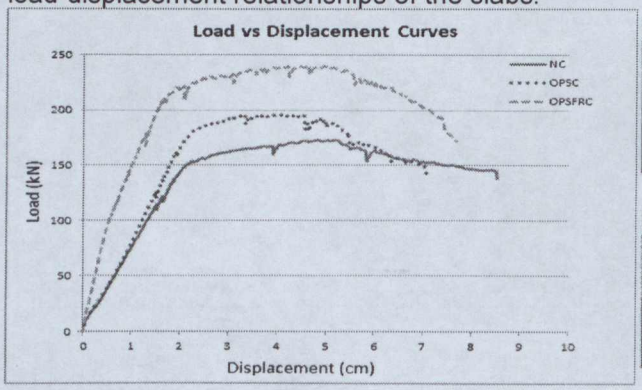

Figure 5: Load-Displacement relationships of the slabs

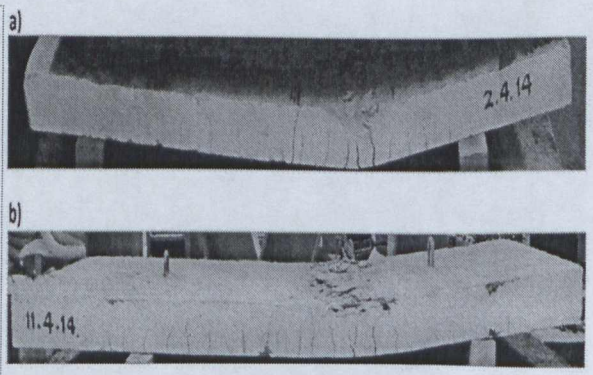

Figure 6: Cracks propagation a) NC slab b) OPSC slab

As shown in Figure 6 multiple flexural cracks are distributed along all NC, and OPSC slabs. Cracks propagate more than half way along the slab thickness and it can be seen that several cracks opened up on the bottom face including concrete crushed on the top face for NC and OPSC slabs.

Summary of the quasi-static test results are given in Table 5. OPSC slabs have load carrying capacity 13% higher than NC. However, NC experienced more displacement than OPSC at both maximum load and failure which displays higher ductility.

Table 5: Quasi-static tests summary

Panel Name	Concrete Type	Maximum Load (kN)	Displacement at Maximum Load (cm)	Displacement at Failure (cm)
C1	Normal Concrete (NC)	173.2	4.8	8.5
C2	Oil Palm Shell Concrete (OPSC)	196.2	4.2	7.0

As shown in Figure 6 multiple flexural cracks are distributed along all NC, and OPSC slabs. Cracks propagate more than half way along the slab thickness and it can be seen that several cracks opened up on the bottom face including concrete crushed on the top face for NC and OPSC slabs.

3.2 Blast test results

Pressure-time, deflection-time and acceleration-time histories were measured for ten blast events in the testing program. Post Blast (PB) inspection was conducted on the slabs after every explosion. These inspections were physical examinations at the blast test site. Based on the measured time histories and PB inspection results, the maximum deflections, permanent deflections, details of cracks and failure modes of each slab are discussed in this section.

3.2.1 NC slabs

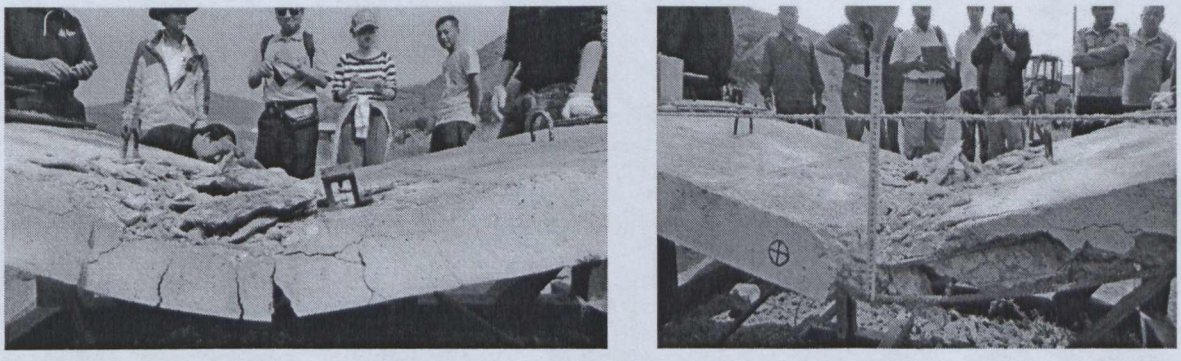

Figure 7: Slab C1 after blast (damaged and formation of shrapnel)

Figure 7 shows slab C1 subjected to explosion of 10 kg charge LVDT data and PB inspection data were not recorded for the NC slabs. Further, the slabs were exposed to small scale distances and they experienced larger accelerations than predicted. Hence, accelerometers were unable to record Acceleration-Time (AT) histories properly. Thus the way that NC slabs were responded to the blast loads is not known. This may cause difficulties to compare NC slab response with the slabs casted by other types of concrete.

3.2.2 OPSC slabs

The recorded Deflection-Time (DT) histories of C2A and C2B slabs are shown in Figure 8. The LVDT did not capture the full DT history for C2A due to 1 kg charge explosion. For 10 kg charge, DT curve has a plateau at approximately 9 cm. The maximum deflection of the slab may be more than 9 cm; however, LVDT was not being able to capture it. PB inspection was reported a permanent deflection of nearly 2 cm for the slab. As per Figure 8 b), the maximum deflection recorded by LVDT for C2B is approximately 7.8 cm. However in the figure for Slab C2B, it can be seen a plateau at the maximum deflection too. Actual deflection might be more than 7.8 cm. But due to the limitations of LVDT, it might not be able to record the deflection more than 7.8 cm. Permanent deflection of slab C2B recorded by LVDT is 4.3 cm. Permanent deflection of slab C2B measured at the site was well

agreed with the LVDT result which indicated the ability of LVDT to measure slab deflections accurately within its acceptable limits. The slab accelerations were more than 50 m/s^2, hence the accelerometers were unable to measure AT curves accurately.

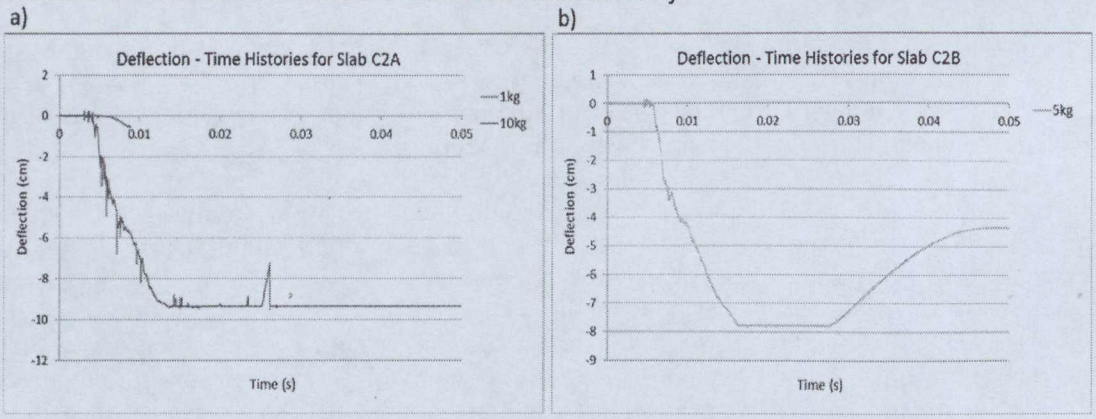

Figure 8: Deflection-Time (DT) history for OPSC slabs a) C2A b) C2B

Figure 9 shows slab C2A subjected to explosion of 10 kg charge. In Figure 9 a), it can be seen that tensile cracks have developed on the bottom face along the slab length which propagates up to three-fourth of depth of the slab. The cracks have opened up, indicating plastic response of the slab. However all the cracks have not spread along the entire width as shown in Figure 9 b). Other than tensile cracks, shear cracks can be observed close to the both supports. Shear cracks at the right support are shown in Figure 9 c). Based on post inspection data, it can be mentioned that slab C2A failed by both flexure and diagonal shear modes.

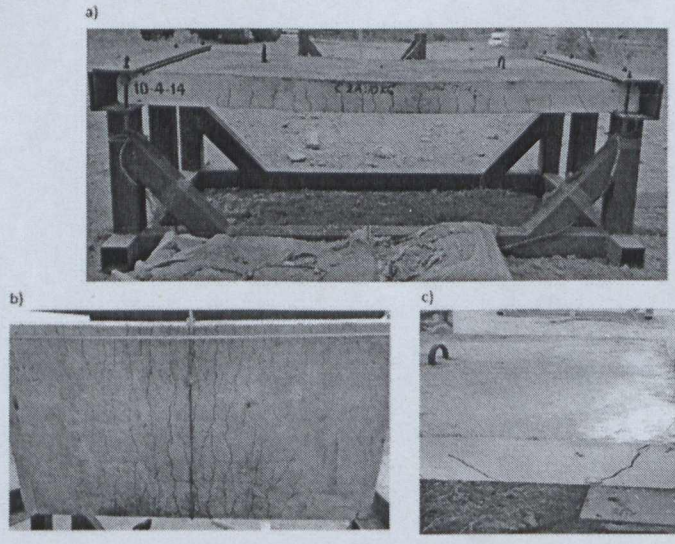

Figure 9: Slab C2A after blast a) side view b) slab bottom c) shear cracks at the support

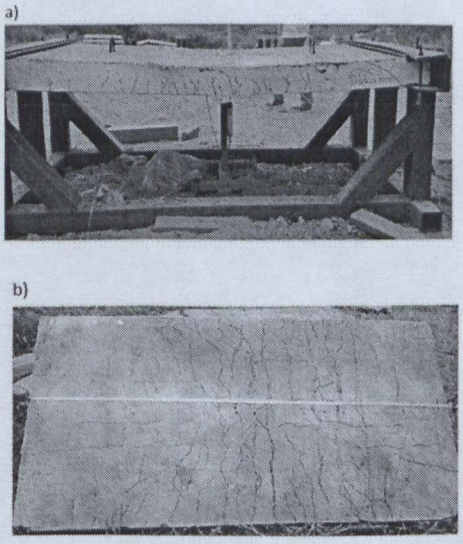

Figure 10: a) side view b) bottom face of slab C2B after blast

Figure 10 shows the PB condition of slab C2B. As shown in Figure a), multiple tensile cracks can be observed along the entire length of the slab. Cracks close to the centre propagated up to 100 mm of slab depth. They opened up about 2 mm wide and evidence for beginning of concrete crushing was exhibited on top face of the slab close to mid-span which means that the slab has experienced plastic response. Shear cracks also can be seen close to the supports in the figure. However the cracks at right support are more visible than at left support. Bottom face of the slab is shown in Figure b) which indicates crack propagation along the width. However, there can be seen some cracks in longitudinal direction as well. Similar to slab C2A, slab C2B also failed by both flexure and diagonal shear modes.

3.2.3 Comparison of the blast test results

Table 6 summarizes the slab responses for blast events to compare the results for each concrete type. As per the summary, LVDT data shows permanent deflections less than 1 cm for slab C2A for 1 kg charge explosions. As mentioned earlier, this can be caused by settlement of the LVDTs. PB inspections were not recorded either any permanent deflections or cracks on both C2A due to 1kg charge explosion. Hence, these slabs can be considered in elastic state as predicted.

Table 6: Comparison of the slab responses to blast loads

Event	Panel Name	Concrete Type	Scaled Distance ($m/kg^{1/3}$)	Charge Weight (kg)	Maximum Deflection (cm) by LVDT	Permanent Deflection (cm)		Maximum Crack Width (cm)	Failure Mode
						by LVDT	by Inspection		
4	C2A	OPSC	1.5	1	0.5	-	-	NA	
5			0.7	10	-	-	2	≈0.2	Flexure and shear
6	C2B		0.88	5	> 7.8	4.3	4	≈0.2	Flexure and shear

Due to 10 kg charge explosions, OPSC slab C2A failed in both flexure and shear with nearly 2 cm permanent deflection. The slab had fine cracks which were approximately 0.2 cm wide along its length. When considering the slab response to 10 kg charge explosion, OPSC slab seems more effective than NC slab.

Flexural cracks were opened up along the length in all the slabs subject to 5kg charge explosion, however they were approximately 1-2 mm in width. As shown in Figure 1, OPSC slab C2B was recorded maximum deflection of 7.8 cm. The permanent deflections which were recorded by LVDT data, agreed well with PB inspection data. OPSC slab had permanent deflection of 4 cm and experienced plastic response.

This is quite contradict to the response for 10 kg charge explosion, which OPSC slab C2A showed better performance than NC slab. Further investigation is needed to understand structural behaviour of OPSC slabs subject to blast load. Also OPSC slabs experienced both flexural and shear cracks.

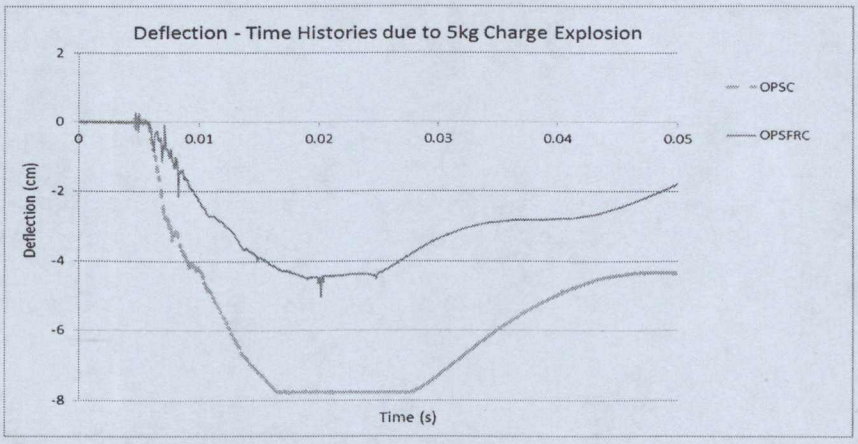

Figure 11: Deflection – Time histories of concrete slabs due to 5kg charge explosion

Because the test data was not recorded for NC slabs, test data from earlier blast tests with quite similar material and blast load properties conducted by the University of Adelaide was used for a comparison with OPS slab test results [18]. These NC slab test data are given in Table 7. Slab 1 in the table was subjected to a blast load of 8.14 kg charge with Scaled Distance (SD) of 1.5 $m/kg^{1/3}$ and it had the maximum deflection of 1.05 cm. For SD 1.5 $m/kg^{1/3}$ blast load, the slabs with OPS had the maximum deflections of less than 1cm as given in Table 6. Even if there was the same peak pressure acting on all the slabs because of the same SD, the impulse on slab 1 was two times larger because of 8 kg charge weight compared to 1 kg charge of OPS slabs in this study [21]. Also, slab 1 has smaller slab thickness than other slabs. There wasn't any visible crack on the slab after the blast which means slab 1 was in elastic state similar to OPS slabs. When comparing the slabs, both NC and OPS slabs were responded in quite similar way for SD 1.5 $m/kg^{1/3}$ blast loads.

Table 7: Normal concrete slab responses to blast loads

Slab No.	Slab Thickness (mm)	Concrete Strength (MPa)	Reinforce Steel Strength (MPa)	Steel Ratio (%)	Charge Weight (kg)	Charge Shape	Standoff Distance (m)	Scaled Distance (m/ $kg^{1/3}$)	Deflection		Reference
									Maximum (cm)	Permanent (cm)	
1	100	39.5	600	1.34	8	Cylindrical	3	1.50	1.05	-	Wu et al. [18]
2	100	39.5	600	1.34	3.5	Cylindrical	1.4	0.93	1.39	-	
3	100	39.5	600	1.34	8	Cylindrical	1.5	0.75	3.89	-	

Slab 2 in Table 7 was subjected to explosion of 3.44 kg charge at SD 0.93 m/$kg^{1/3}$. The recorded maximum deflection is 1.39 cm and fine tensile cracks were observed along the length of the slab [18]. There was not any permanent deflection recorded. Even though in Figure 11a) it can be seen tensile cracks at the bottom of slab 2, it is unlikely that the ultimate moment in the slab reached [18]. Slab 2 had larger reinforced steel ratio than OPS slabs which increases its flexural strength but smaller thickness of the slab affected negatively on rigidity of the slab. For 5 kg charge loading at SD 0.88 m/$kg^{1/3}$, OPS slabs reached to plastic state. OPS slabs were subjected to a larger blast load due to a lager charge weight and smaller SD than slab 2. Even if the charge was cylindrical in shape for both cases, the charge was oriented vertically for OPS slabs, which applied intensify load specially at near field (at small SD) than cylindrical charges which are oriented horizontally as for slab 2 [22, 23].

As given in Table 7 due to 8 kg charge blast when SD 0.75 m/$kg^{1/3}$, slab 3 has undergone the maximum deflection of 3.89 cm and there was tensile cracks along the slab length which propagates significant depth of the slab as shown in the Figure 11b). Cracks were opened, indicating a plastic or post-yield response however any permanent deflection were not observed [18]. OPS slabs were severely damaged by blast load due to 10 kg charge at SD 0.75 m/$kg^{1/3}$ except OPSC slab, which had better response than slab 3 even for a quite larger blast load.

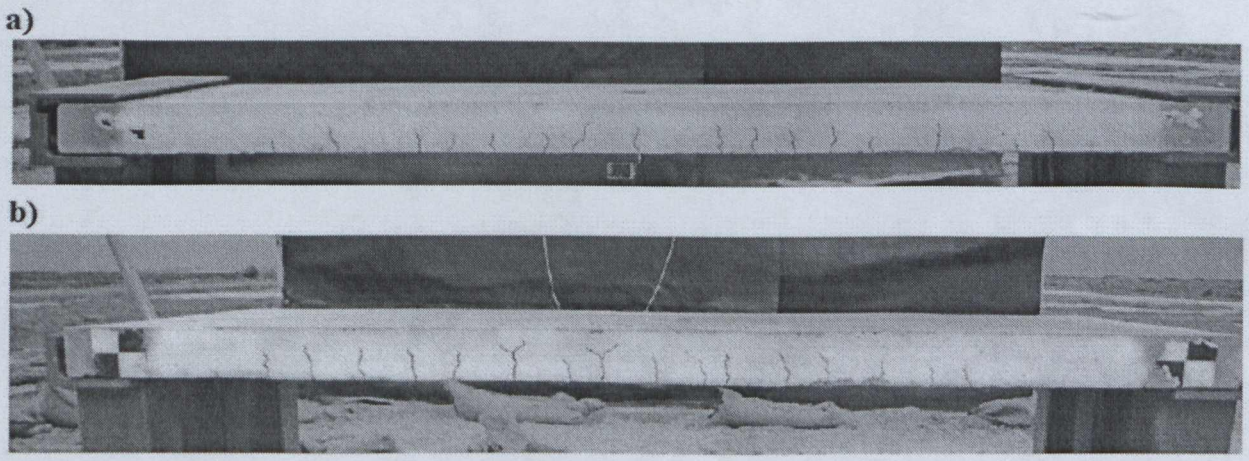

Figure 11: Cracks in a) slab 2 and b) slab 3 [18]

4. CONCLUSIONS

In this blast testing program, concrete slabs casted by NC, and OPSC were tested for quasi-static load and blast loads with different charge weights that located at 1.5 m distance away from the slabs.

In quasi-static tests, OPSC slabs had higher load carrying capacity compare to NC slab however OPSC and NC slabs have similar energy absorption capacity.

For 1 kg charge explosions, the slab responses are in elastic state and PB inspections of the slabs didn't record either cracks or permanent deflection for all concrete types.

By referring LVDT data for 5 kg charge explosions, OPSC slab had the highest maximum deflection and permanent deflection. However as per PB inspection data, for 10 kg charge explosion OPSC slab had low permanent deflection and crack widths.

OPS slabs showed quite similar response to blast load as NC slabs. This indicates that OPS is an effective alternative for granite aggregate as a coarse aggregate in concrete when resisting both quasi-static and blast loads.

5. ACKNOWLEDGEMENTS

The financial support provided by University of Malaya under the grant RP037C-15AET *"Synthesis of Nano Silica, Alumina and Tio2 in the Development of Geopolymer of Concrete Using Local Waste"* is gratefully acknowledged.

REFERENCES

[1]. Meyer, C., *The greening of the concrete industry.* Cement and Concrete Composites, 2009. **31**(8): p. 601-605.
[2]. Choi, J., et al., *Influence of fiber reinforcement on strength and toughness of all-lightweight concrete.* Construction and Building Materials, 2014. **69**: p. 381-389.
[3]. Chen, B. and J. Liu, *Contribution of hybrid fibers on the properties of the high-strength lightweight concrete having good workability.* Cement and Concrete Research, 2005. **35**(5): p. 913-917.
[4]. Mo, K.H., et al., *The effect of steel fibres on the enhancement of flexural and compressive toughness and fracture characteristics of oil palm shell concrete.* Construction and Building Materials, 2014. **55**(0): p. 20-28.
[5]. Teo, D.C.L., M.A. Mannan, and J.V. Kurian, *Flexural behaviour of reinforced lightweight concrete beams made with Oil Palm Shell (OPS).* Journal of Advanced Concrete Technology, 2006. **4**(3): p. 459-468.
[6]. Mohammed, B.S., W.L. Foo, and M. Abdullahi, *Flexural strength of palm oil clinker concrete beams.* Materials & Design, 2014. **53**: p. 325-331.
[7]. Mahmud, H., M.Z. Jumaat, and U.J. Alengaram, *Influence of sand/ cement ratio on mechanical properties of palm kernel shell concrete.* Journal of Applied Sciences, 2009. **9**(9): p. 1764 - 1769.
[8]. Mannan, M.A. and C. Ganapathy, *Engineering properties of concrete with oil palm shell as coarse aggregate.* Construction and Building Materials, 2002. **16**(1): p. 29-34.
[9]. Mo, K.H., et al., *Impact resistance of hybrid fibre-reinforced oil palm shell concrete.* Journal of Construction and Building Materials, 2014. **50**: p. 499-507.
[10]. Mannan, M., et al., *Quality improvement of oil palm shell (OPS) as coarse aggregate in lightweight concrete.* Building and Environment, 2006. **41**(9): p. 1239-1242.
[11]. Yap, S.P., et al., *Flexural toughness characteristics of steel–polypropylene hybrid fibre-reinforced oil palm shell concrete.* Materials & Design, 2014. **57**: p. 652-659.
[12]. Mo, K.H., et al., *Impact resistance of hybrid fibre-reinforced oil palm shell concrete.* Construction and Building Materials, 2014. **50**(0): p. 499-507.
[13]. Alengaram, U.J., M.Z. Jumaat, and H. Mahmud, *Ductility behaviour of reinforced palm kernel shell concrete beams.* European Journal of Scientific Research, 2008. **23**(3): p. 406-420.
[14]. Onoue, K., H. Tamai, and H. Suseno, *Shock-absorbing capability of lightweight concrete utilizing volcanic pumice aggregate.* Construction and Building Materials, 2015. **83**: p. 261-274.
[15]. Bischoff, P., K. Yamura, and S. Perry. *Polystyrene aggregate concrete subjected to hard impact.* in *Institution of Civil Engineers, Proceedings, Pt 2.* 1990.
[16]. Yap, S.P., et al., *Effect of fibre aspect ratio on the torsional behaviour of steel fibre-reinforced normal weight concrete and lightweight concrete.* Engineering Structures, 2015. **101**: p. 24-33.
[17]. Luccioni B M, Ambrosini R D, and Danesi R F, *Analysis of building collapse under blast loads.* Engineering Structures, 2003. **26**: p. 63-71.
[18]. Wu, C., et al., *Blast testing of ultra-high performance fibre and FRP retrofitted concrete slabs.* Engineering Structures, 2009. **31**: p. 2060-2069.
[19]. Dragos J., et al., *Derivation of normalized pressure impuse curves for flexural ultra high performance concrete slabs.* Journal of Structural Engineering, ASCE, 2013. **139**: p. 875-885.
[20]. Yap, S.P., et al., *Flexural toughness characteristics of steel-polypropylene hybrid fibre-reinforced oil palm shell concrete.* International Journal of Materials and Design, 2014. **57**: p. 652-659.
[21]. Criteria, U.F., *UFC 3-340-02 (2008), Structures to resist the effects of accidental explosions.* Department of Defense, USA.
[22]. Wu, C., et al., *Investigation of air-blast effects from spherical and cylindrical shaped charges.* International Journal of Protective Structures, 2010. **1**(3): p. 345 - 362.
[23]. Weerasingha, M.N., et al. *Critical scaled distances of spherical vs cylindrical charge shape effects for external, fully vented confined and fully confined blasts.* in *5th International Conference on Protection of Structures against Hazards* 2012. Singapore.